A numerical study of the similarity of fully developed turbulent flows in orthogonally rotating square ducts and stationary curved square ducts

Received November 2000
Accepted December 2001

Gong Hee Lee
Department of Mechanical Engineering, Pohang University of Science and Technology, Korea
Je Hyun Baek
Professor, Department of Mechanical Engineering, Pohang University of Science and Technology, Korea

Keywords *Flow, Numerical methods*

Abstract *A numerical study of a quantitative analogy of fully developed turbulent flow in a straight square duct rotating about an axis perpendicular to that of the duct and a stationary curved duct of square cross-section was carried out. In order to compare the two flows, the dimensionless parameters* $K_{TR} = Re^{1/4}/\sqrt{Ro}$ *and the Rossby number,* $Ro = w_m/\Omega d_h$*, in the rotating straight duct flow corresponded to* $K_{TC} = Re^{1/4}/\sqrt{\lambda}$ *and the curvature ratio,* $\lambda = R/d_h$*, in the stationary curved duct flow, so that they had the same dynamical meaning as those parameters for fully developed laminar flow. For the large values of Ro or* λ*, the flow field satisfied the "asymptotic invariance property"; there were strong quantitative similarities between the two flows, such as in the flow patterns and friction factors for the same values of* K_{TR} *and* K_{TC}*. Based on these similarities, it is possible to predict the flow characteristics in rotating ducts by considering the flow in stationary curved ducts, and vice versa.*

Nomenclature

d = pipe diameter
d_h = hydraulic diameter of the duct
f = Fanning friction factor
f_0 = friction factor for a stationary straight duct flow
K_{LR} = dimensionless parameter for laminar flow in a rotating duct $= Re/\sqrt{Ro}$
K_{LC} = dimensionless parameter for laminar flow in a curved duct or Dean number $= Re/\sqrt{\lambda}$
K_{TR} = dimensionless parameter for turbulent flow in a rotating duct $= Re^{1/4}/\sqrt{Ro}$
K_{TC} = dimensionless parameter for turbulent flow in a curved duct $= Re^{1/4}/\sqrt{\lambda}$

This work was partially supported by the Brain Korea 21 Project and the authors gratefully thank Dr. Ishigaki for some valuable comments during the "Winter Institute Program" supported by the Japan-Korea Industrial Technology Cooperation Foundation.

International Journal of Numerical Methods for Heat & Fluid Flow, Vol. 12 No. 3, 2002, pp. 241-257.

DOI 10.1108/09615530210422901

k = turbulence kinetic energy
p = static pressure
p^* = modified pressure $= p - \frac{1}{2}\rho\Omega^2(x^2 + z^2)$
R = mean radius of curvature
Re = Reynolds number $= w_m d_h / v$
Re_T = turbulence Reynolds number $= k/\omega\nu$
Ro = Rossby number $= w_m/\Omega d_h$
S_{ij} = strain-rate tensor
u, v, w = velocity components in the direction of x, y, z
V_{sa} = secondary axial velocity $= w_{rot} - w_{norot}$ for a rotating straight duct $= w_{curv} - w_{norot}$ for a stationary curved duct
w_m = mean velocity
w_τ = friction velocity $= \sqrt{\tau_w/\rho}$
Y = normal distance from the wall
y^+ = dimensionless wall distance $= w_\tau Y/\nu$

Greek symbols
Ω = angular velocity
δ_{ij} = Kronecker delta
λ = curvature ratio $= R/d_h$
μ = laminar viscosity of the fluid
μ_t = eddy viscosity
ν = kinematic viscosity of the fluid
ρ = density of the fluid
τ_{ij} = Reynolds stress tensor
τ_w = wall shear stress
ω = specific dissipation rate of the turbulence kinetic energy

Introduction

Fluid flow in rotating and curved ducts is of interest because of its relevance to various engineering applications. This includes flow through the cooling passages of turbine blades, turbomachinery blade passages, heat exchangers, and refrigeration equipment. These examples all feature secondary flow effects due to rotation and curvature. Such secondary flow not only reduces the volumetric flow rate for a fixed pressure difference, but also redistributes the axial velocity field.

In fully developed flow through a straight duct rotating about an axis normal to that of the duct, the Coriolis force throws fast-moving core flow in the direction of the cross product of the mean velocity and the rotation vectors. The near-wall flow is driven from the pressure side to the suction side of the duct to preserve continuity along the wall regions. The onset of this secondary flow increases the average values of the friction factor and the wall heat transfer rate. In their experimental studies of the strong effect of rotation on the turbulent wall boundary layers in a rotating rectangular duct, Hill and Moon (1962) showed that on the pressure side of the duct, the rate of turbulent mixing is increased and the boundary layer becomes considerably thinner, while the reverse occurs on the suction side. Moore (1967) revealed that the influence of rotation on velocity profiles, wall shear stresses, and turbulence distributions is strongly dependent on the aspect ratio (height/width). The effect of rotation is quite large at low aspect ratios, whereas much smaller effects are observed at high ratios. Johnston *et al.* (1972) used an extremely narrow channel in which the central flow region was unaffected by corner secondary flows. They found that the body forces associated with rotation severely modify the mean flow and turbulence fields. On the suction side of the channel, turbulence activity is diminished, and eventually suppressed at high rotation rates, such that the flow becomes laminar again at relatively high Reynolds numbers. On

the contrary, turbulence activity is significantly enhanced and the turbulent eddies aggregate into roll cells on the pressure side. Iacovides and Launder (1991) numerically showed that the secondary flow experiences a transition from the well-known double-vortex structure to a more complex four-vortex structure due to flow instabilities on the pressure side at higher rotational speeds.

Since longitudinal curvature and spanwise rotation produce similar effects, analogous flow patterns can be observed in the fully developed flow of stationary curved ducts. When a viscous fluid flows through a curved duct, the streamline curvature generates a centrifugal force that acts normal to the main flow and produces a secondary flow. This double counter-rotating secondary flow causes the symmetric and quasi-parabolic axial velocity profile to become asymmetric, shifting the location of the maximum axial velocity outward. Humphrey *et al.* (1981) showed that the stabilizing effects due to the convex curvature of the inner wall of the duct are responsible for lowering the turbulence intensity there, whereas the destabilizing effects due to the concave curvature at the outer wall increase it. Using LDV (Laser-Doppler Velocimetry) measurements, Taylor *et al.* (1982) found that the magnitude of secondary flow in a "weakly curved" duct is much smaller than that in a "strongly curved" duct, but its effect is more important to the streamwise flow development because of the lower streamwise pressure gradients.

Although a few studies have attempted to verify the similarity of the two flows, their approaches were mainly qualitative. For example, Trefethen (1957) showed that variation in the friction factor due to the secondary flow patterns in both rotating and curved pipes can be expressed in terms of the Reynolds number and a dimensionless parameter characterizing each flow, but he did not provide a theoretical explanation. Ito and Nanbu (1971) and Ito (1959) derived dimensionless parameters for these flows using an integral method, but they did not mention any relationships between these parameters. Ishigaki (1994, 1996) introduced dimensionless parameters to demonstrate the quantitative analogy between two flows in a circular pipe, and obtained satisfactory results. In a previous paper (Lee and Baek, 2001), we confirmed the quantitative analogy of fully developed laminar flows in orthogonally rotating straight ducts and stationary curved ducts of square cross-section, using the dimensionless parameters suggested by Ishigaki (1994). Our current objective is to show that this quantitative analogy is also valid for fully developed turbulent flow using the similarity parameters that have the same dynamical meaning as those of the fully developed laminar flows. A low Reynolds number $k - \omega$ turbulence model and a higher order discretization scheme are used to predict the flow fields reliably. Based on the results, it is possible to predict the flow characteristics in rotating ducts by considering the flow in stationary curved ducts, and vice versa.

Governing equations

A Cartesian coordinate system fixed to a straight duct that rotates about y-axis at a constant angular velocity Ω (Figure 1(a)), and a cylindrical coordinate system in which the radius of curvature along the duct centerline is represented by R (Figure 1(b)), are used for flow analysis in a rotating duct and a curved duct of square cross-section, respectively. The velocity components in the direction of increasing (x, y, z) are denoted by (u, v, w). Here, u and v are the velocity components of secondary flow in a cross-section, while w stands for the primary flow. Since u, v, and w are independent of the z-direction in the fully developed region, the equations of continuity and mean momentum for incompressible, turbulent flow can be written as follows:

Continuity

$$\frac{\partial u}{\partial x} + \frac{\partial v}{\partial y} = 0 \tag{1}$$

Mean momentum

$$\frac{\partial}{\partial t}(\rho\phi) + \frac{\partial}{\partial x}\left[\rho u\phi - (\mu + \mu_t)\frac{\partial \phi}{\partial x}\right] + \frac{\partial}{\partial y}\left[\rho v\phi - (\mu + \mu_t)\frac{\partial \phi}{\partial y}\right] = P_\phi + S_\phi \tag{2}$$

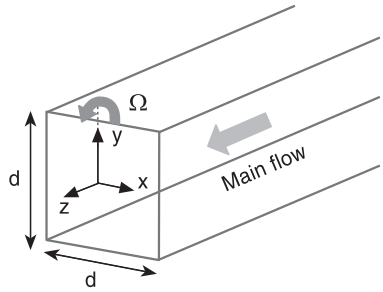

(a) Rotating straight duct

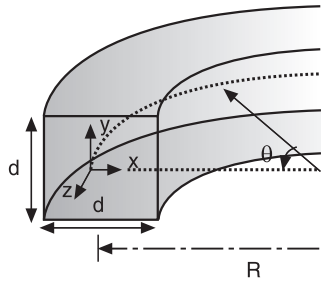

(b) Stationary curved duct

Figure 1.
The configuration and the coordinate system for flow analysis

where ϕ represents u, v, or w. The pressure gradient term, P_ϕ, and the body force term, S_ϕ, for both flows are given in Table I. In a rotating duct flow, p^* is the modified pressure given by

$$p^* = p - \frac{1}{2}\rho\Omega^2(x^2 + z^2) \tag{3}$$

Governing Equations (1) and (2) are the limiting forms for both "weakly rotating" (where the effect of rotation is negligible) and "weakly curved" (where the effect of curvature is negligible) duct flows.

Since the conventional high Reynolds number $k - \varepsilon$ model (Launder and Spalding, 1974) is unable to resolve the near-wall motion that is responsible for the development of the Coriolis and curvature driven secondary flow, the low Reynolds number $k - \omega$ model (Wilcox, 1994) is used. This model reliably predicts flows with adverse pressure gradient, rotation, and streamline curvature (Wilcox, 1993; Stephens and Shih, 1999; Song *et al.*, 2001). In addition, this model has significant advantages in numerical stability in that it does not employ any type of damping functions. The /for the turbulence kinetic energy, k, and specific dissipation rate, ω, are

$$\frac{\partial}{\partial t}(\rho k) + \frac{\partial}{\partial x_j}(\rho u_j k) = \tau_{ij}\frac{\partial u_i}{\partial x_j} - \beta^*\rho\omega k + \frac{\partial}{\partial x_j}\left[\left(\mu + \frac{\mu_t}{\sigma_k}\right)\frac{\partial k}{\partial x_j}\right] \tag{4}$$

$$\frac{\partial}{\partial t}(\rho\omega) + \frac{\partial}{\partial x_j}(\rho u_j \omega) = \alpha\frac{\omega}{k}\tau_{ij}\frac{\partial u_i}{\partial x_j} - \beta\rho\omega^2 + \frac{\partial}{\partial x_j}\left[\left(\mu + \frac{\mu_t}{\sigma_\omega}\right)\frac{\partial \omega}{\partial x_j}\right] \tag{5}$$

where the eddy viscosity, μ_t, is related to k and ω by

$$\mu_t = \alpha^*\rho k/\omega \tag{6}$$

and the Reynolds stress tensor, τ_{ij}, the strain-rate tensor, S_{ij}, and the turbulence Reynolds number, Re_T, are defined as follows:

$$\tau_{ij} = 2\mu_t\left(S_{ij} - \frac{1}{3}\frac{\partial u_k}{\partial x_k}\delta_{ij}\right) - \frac{2}{3}\rho k\delta_{ij}, \quad S_{ij} = \frac{1}{2}\left(\frac{\partial u_i}{\partial x_j} + \frac{\partial u_j}{\partial x_i}\right), \quad Re_T = k/\omega\nu \tag{7}$$

	P_ϕ		S_ϕ	
ϕ	Rotating flow	Curved flow	Rotating flow	Curved flow
u	$-\frac{\partial p^*}{\partial x}$	$-\frac{\partial p}{\partial x}$	$2\rho\Omega w$	$\frac{\rho w^2}{R+x}$
v	$-\frac{\partial p^*}{\partial y}$	$-\frac{\partial p}{\partial y}$	0	0
w	$-\frac{\partial p^*}{\partial z}$	$-\frac{\partial p}{\partial z}$	$-2\rho\Omega u$	$-\frac{\rho uw}{R+x}$

Table I. The pressure gradient and body force term for the variable ϕ

Furthermore, α, α^*, β, β^*, σ_k, and σ_ω are closure coefficients whose values are summarized in Table II.

$$\alpha^* = \frac{\alpha_0^* + Re_T/R_k}{1 + Re_T/R_k}, \quad \alpha = \frac{5}{9}\frac{\alpha_0 + Re_T/R_\omega}{1 + Re_T/R_\omega}\frac{1}{\alpha^*}, \quad \beta^* = \frac{9}{100}\frac{5/18 + (Re_T/R_\beta)^4}{1 + (Re_T/R_\beta)^4} \tag{8}$$

Similarity parameters

Most previous studies on turbulent flow in rotating or stationary curved ducts used the Reynolds number, $Re = w_m d_h/\nu$, to describe the characteristics of the flows. For example, Lezius and Johnston (1976), Iacovides and Launder (1991), and Younis (1993) introduced two dimensionless parameters, Re and $1/Ro$, to characterize turbulent flow in a rotating duct, while Patankar *et al.* (1975), Taylor *et al.* (1982), and Hur *et al.* (1990) used Re and λ as the corresponding parameters in a stationary curved duct. However, Re does not involve the effects of either rotation or curvature. In a previous paper (Lee and Baek, 2001) dealing with a quantitative analogy of fully developed laminar flow in ducts of the same configuration, a pair of dimensionless parameters, K_{LR} and Ro, in a rotating duct flow was used as a set corresponding to K_{LC} and λ in a stationary curved duct flow. For laminar flows in orthogonally rotating ducts, the pair of dimensionless parameters K_{LR} and Ro can be drived as follows (for a circular pipe flow, see Ishigaki (1994)):

$$K_{LR} = (F_i F_r)^{1/2}/F_{Lv} = Re/\sqrt{Ro} \tag{9}$$

$$Ro = F_i/F_r = w_m/\Omega d_h \tag{10}$$

where $F_i \sim \rho w_m^2/d_h$, $F_r \sim \rho\Omega w_m$ and $F_{Lv} \sim \mu w_m/d_h^2$ represent the inertia, Coriolis, and laminar viscous forces, respectively. In Equation (9), K_{LR} stands for the Reynolds number based on the velocity scale of secondary flow in a rotating duct, $U_{SR} = w_m/\sqrt{Ro}$, and the length scale d_h. The Rossby number, Ro, can be considered as a measure of the relative strength of the inertia force to the Coriolis force acting on the fluid. In a similar way, for laminar flows in stationary curved ducts, the pair of dimensionless parameters K_{LC} and λ can be obtained by replacing the Coriolis force in K_{LR} and Ro with the centrifugal force.

Table II. Turbulence model constants

σ_k	σ_ω	α_0	α_0^*	β	R_k	R_ω	R_β
2.0	2.0	1/10	1/40	3/40	6.0	2.7	8.0

$$K_{\mathrm{LC}} = (F_i F_{\mathrm{c}})^{1/2}/F_{\mathrm{Lv}} = Re/\sqrt{\lambda} \tag{11}$$

$$\lambda = F_i/F_{\mathrm{c}} = R/d_{\mathrm{h}} \tag{12}$$

where $F_{\mathrm{c}} \sim \rho w_m^2/R$ is the centrifugal force. In Equation (11), K_{LC} is the Dean number and provides a measure of the intensity of the secondary flow. The curvature ratio, λ, represents the ratio of the inertia force to the centrifugal force. In order to find the similarity parameters in turbulent flows that have the same dynamical meaning as K_{LR} and K_{LC} for laminar flows, a different approach for estimating the viscous force is needed. The method used here is similar to that used by Ishigaki (1996) for a circular pipe flow, except that it employs the hydraulic diameter, d_{h}, instead of the diameter of the pipe, d. In fully developed turbulent flows through a straight pipe, the wall shear stress τ_{w} can be estimated from the Blasius resistance formula (Schlichting, 1979). Since the friction factor for a circular pipe agrees with that for a duct with a square cross-section, the turbulent viscous force, F_{Tv}, can be approximated as $F_{\mathrm{Tv}} \sim \tau_{\mathrm{w}}/d_{\mathrm{h}} \sim \rho w_m^{7/4} \nu^{1/4} d_{\mathrm{h}}^{-5/4}$. Applying this to Equations (9) and (11), the similarity parameters in turbulent flow that correspond to K_{LR} and K_{LC} for laminar flow can be obtained as follows:

$$K_{\mathrm{TR}} = (F_i F_r)^{1/2}/F_{\mathrm{Tv}} = (Re)^{1/4}/\sqrt{Ro} \tag{13}$$

$$K_{\mathrm{TC}} = (F_i F_{\mathrm{c}})^{1/2}/F_{\mathrm{Tv}} = (Re)^{1/4}/\sqrt{\lambda} \tag{14}$$

The second parameters Ro and λ have the same forms as in laminar flow, since the inertia force and body force do not include the viscous force term. For large values of Ro or λ, flow features are independent of these parameters. This important property, the so-called "asymptotic invariance property", has been discussed by several authors. For examples, Ito and Nanbu (1971) showed that their experimental results for rotating pipe flow conformed satisfactorily to a single curve for $Ro \geq 10$. Moreover, Ito's study (1959) of the finite curvature effects manifested that the effects of λ were practically negligible for $\lambda \geq 8$. In summary, in analogy to laminar flow, K_{TR} or K_{TC} is the sole governing parameter in each turbulent flow and similarity between the two flows is expected for the range of values of Ro or λ that satisfy the "asymptotic invariance property".

Numerical method

In general, a numerical solution of the Navier-Stokes equations is expensive, because the resulting discrete equations for the velocity components and pressure are coupled. A fractional step method can alleviate this difficulty by decoupling the solution of the momentum equations from the solution of the continuity equation (Harlow and Welch, 1965; Chorin, 1968; Rosenfeld *et al.*, 1991; Lee *et al.*, 2001). In the present method, the calculation is carried out in

two steps. The first step (the convection-diffusion step) solves for an intermediate velocity field (with the pressure gradients omitted) by advancing the momentum equations in time using an implicit ADI method. Then, in order to obtain a divergence-free velocity field, the velocities are corrected by the pressure gradients in the next time step until the continuity equation is satisfied (the continuity step). For steady flow, the solution is advanced in pseudo-time until a converged solution is obtained. The viscous and pressure gradient terms are discretized using second-order accurate central differencing, while second-order accurate upwind differencing is used to minimize the cross-stream numerical diffusion for the convective term. The turbulence model equations are treated in a similar way to the momentum equations. To accelerate the convergence of the solution on the steady state, locally varying time steps are applied to both the Navier-Stokes and turbulence model equations. The use of a non-staggered grid simplifies the implementation of boundary conditions and reduces the additional storage requirements of variables. Convergence criteria are set by 6 orders of residual drop of the solution variables between the current and previous time step. A more detailed descriptions of the numerical scheme can be found in Constantinescu and Patel (1998). At the wall, the no-slip boundary condition is applied. All velocity components and the turbulence kinetic energy, k, are set to zero. For the specific dissipation rate, ω, the following boundary condition proposed by Menter (1993) is used.

$$\omega = 60\nu/\beta(\Delta y)^2 \tag{15}$$

where Δy is the normal distance from the wall to the first grid point. Compared with Wilcox's original form (1993), this condition is much easier to implement and e nsures the same accuracy. Due to the symmetric configuration of the flow, the computation is only performed in a half-domain of the cross-section with the symmetry boundary condition. On the cross-sectional plane, a non-uniform 89×45 grid with clustering at the near wall region is used. The node closest to the wall lies below $y^+ = 1$ and at least 6 nodes cover a region within $y^+ < 10$ to resolve the near-wall flow properly. Computations for a wide range of K_T are carried out by fixing the Reynolds number at 2×10^4 and changing the Rossby number or curvature ratio within the range of Ro or $\lambda > 8$.

Results and discussion

General flow patterns

For the same three values of K_{TR} and K_{TC}, Figure 2 shows the non-dimensionalized axial velocity contours, secondary velocity vectors, and streamlines. The upper half of the duct cross-section shows curved duct flow, while the lower half shows rotating duct flow. The pressure and suction sides in rotating duct flow correspond to the outer (convex) and inner (concave) walls, respectively. For rotating duct flow, as the magnitude of K_{TR} increases,

the high-momentum fluid, originally in the central core, is convected to the pressure side of the duct, significantly reducing the thickness of the boundary layers along the pressure and bottom sides, while the low-momentum fluid accumulates along the suction side, causing the boundary layer thickness to increase. The configurations of the secondary flow also change. The existing double-vortex pattern breaks down into an asymmetric structure of four counter-rotating vortices, due to the flow instabilities on the pressure side (Figure 2(c)). In the case of stationary curved duct flow, the inviscid flow near the axis of the duct, which has the highest velocity, is subjected to a larger centrifugal force than the slower-moving fluid near the duct walls; consequently, the location of the maximum axial velocity shifts toward the outer wall of a curved duct. Similar to rotating duct flow, owing to an imbalance between the radial pressure gradient and the centrifugal force, an additional vortex pair appears near the outer wall for large K_{TC} (Figure 2(c)). In conclusion, the two flows show similar patterns for each value of K_T.

The effect of rotation on the flow can be analyzed effectively using the "secondary axial velocity", V_{sa}, defined as the difference between the profiles of axial velocity with and without rotation, as shown in Figure 3. The concept of "secondary axial velocity" can be used identically in a stationary curved duct flow to examine the curvature effect. For $K_T = 3.76$, due to the occurrence of flow instability, the peak velocity drops considerably and shifts towards the center of the duct, resulting in a large negative value of V_{sa} near the pressure side (or outer wall).

The primary velocity profiles along the horizontal centerline of the duct are plotted with the wall-law coordinates in Figure 4. For a smooth wall, the velocity distribution near the wall follows the "law of the wall"

$$\frac{w}{w_\tau} = \frac{1}{\kappa}\ln y^+ + B \tag{16}$$

where w_τ is the friction velocity at the wall, and the constants κ and B take the values 0.42 and 5.45, respectively (Chen and Patel, 1988). Due to the asymmetry of the flow field induced by the effect of rotation or curvature, the friction velocities differ on the pressure and suction sides of the duct. On the unstable pressure side, the enhanced turbulent activity increases the level of wall shear stress, while the reverse occurs on the stabilized suction side, where turbulent activity is diminished. The present prediction shows good agreement with Moore's experimental data (1967).

Friction factor

One of the most important practical aspects of duct flow is an estimate of the friction factor. Ito and Nanbu (1971) used the parameter $K_t = Re/Ro^2$, which corresponds to K_{TR}^4 for rotating pipe flow, and Ito (1959) introduced the dimensionless parameter $Re(d/2R)^2$, which corresponds to K_{TC}^4 for

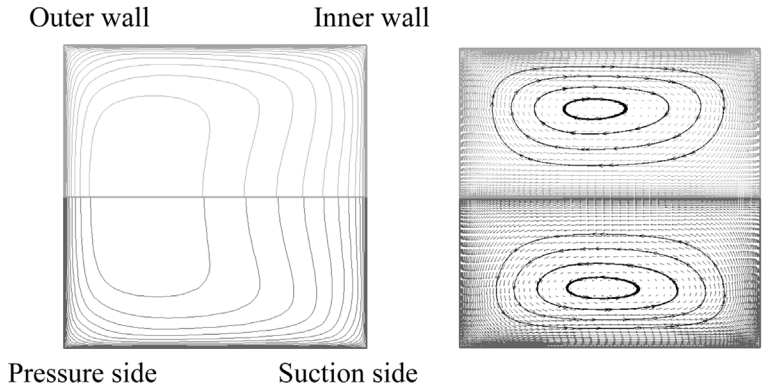

(a) K_T=1.52

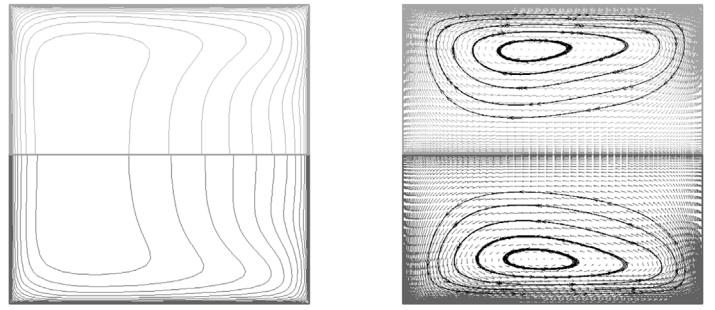

(b) K_T=2.91

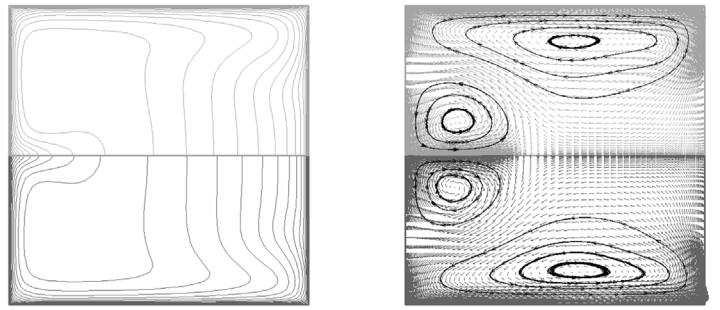

(c) K_T=3.76

Figure 2.
Axial velocity contours (left), secondary velocity vectors and streamlines (right) at $Re = 20{,}000$. (upper: stationary curved duct, lower: rotating straight duct)

curved pipe flow, in order to suggest empirical formulas for the friction factors used to compute the pressure losses for fully developed turbulent flow. The suggested formulas expressed in terms of K_T have the following forms:

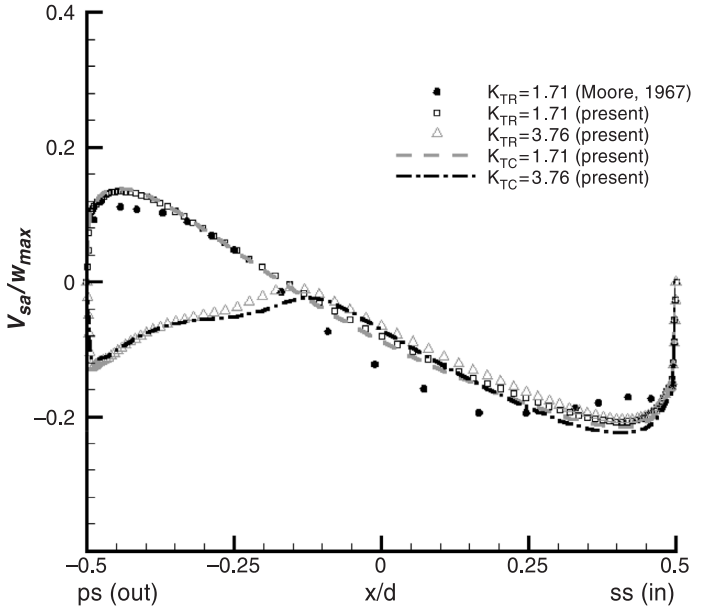

Figure 3.
Secondary axial velocity profiles along the horizontal centerline of the duct at $Re = 20{,}000$

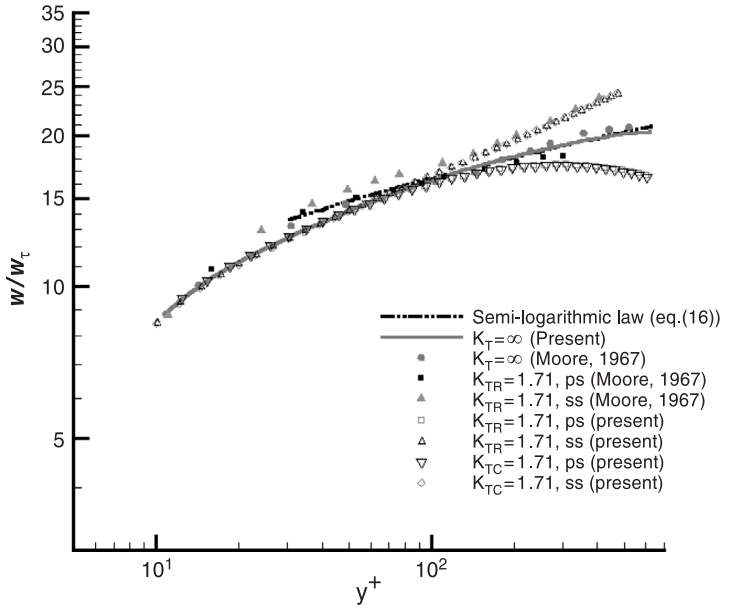

Figure 4.
Comparison of velocity profiles with law of the wall at $Re = 20{,}000$

For rotating straight pipes:

$$\bar{f}/\bar{f}_0 = 0.942 + 0.058K_{\mathrm{TR}}^{1.128} \quad 1 < K_{\mathrm{TR}} < 4.73 \tag{17}$$

For stationary curved pipes:

$$\bar{f}/\bar{f}_0 = 0.962 + 0.065K_{\mathrm{TC}} \quad 0.61 < K_{\mathrm{TC}} < 5.89 \tag{18}$$

For large values of K_{TR} or K_{TC}, they can be simplified as:

For rotating straight pipes;

$$\bar{f}/\bar{f}_0 = 0.924K_{\mathrm{TR}}^{1/5} \quad K_{\mathrm{TR}} > 1.97 \tag{19}$$

For stationary curved pipes;

$$\bar{f}/\bar{f}_0 = 0.933K_{\mathrm{TC}}^{1/5} \quad K_{\mathrm{TC}} > 2.21 \tag{20}$$

where $\bar{f}/\bar{f}_0$ is the ratio of the average friction factors of these two flows normalized by the corresponding value $\bar{f}_0$ for a stationary straight pipe. Comparison of these empirical formulas (Equations (17)–(20)) clearly shows the similarity of the two flows in circular pipes (Figure 5).

In order to verify whether the coincidence of the friction factor is realized for square ducts, the average friction factors on both sides and the overall side are plotted in Figure 6. The top (or bottom) and overall side average values of f/f_0 show a much steeper increase with K_{T} than those of the pressure side. The predicted friction factors for the two flows concur and show good agreement

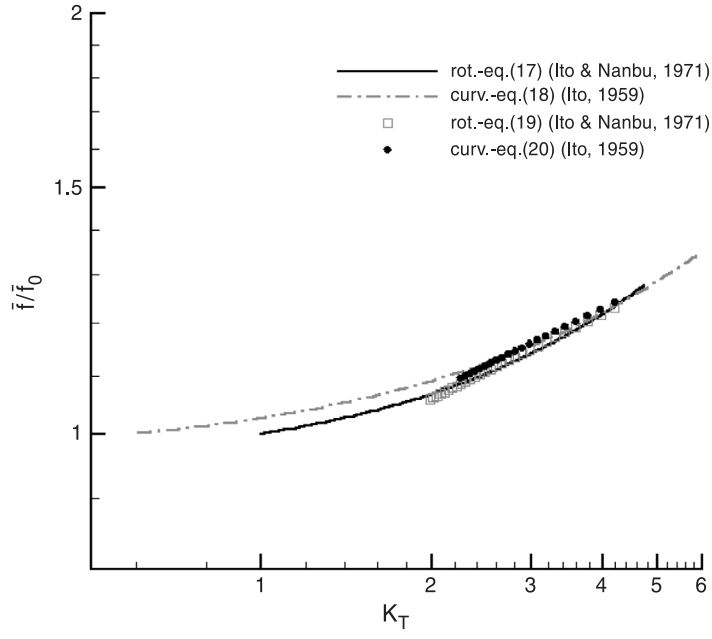

Figure 5.
Friction factor ratio

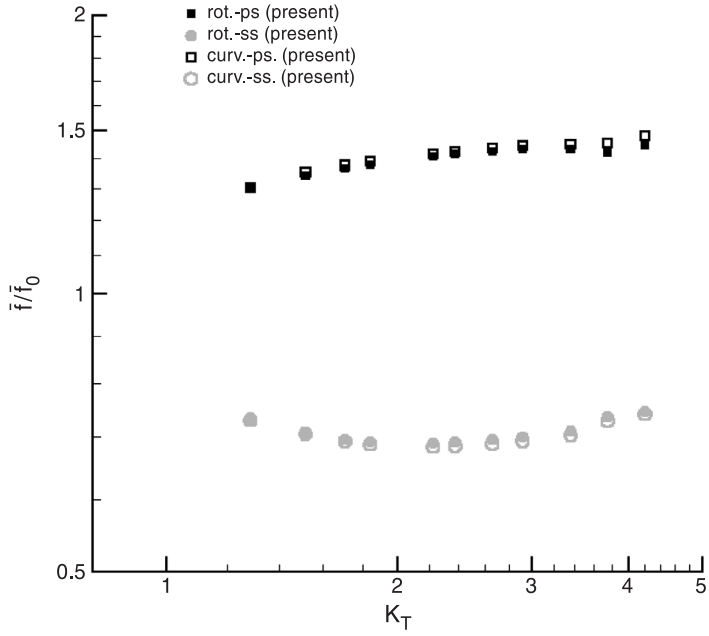

(a) Pressure & suction side

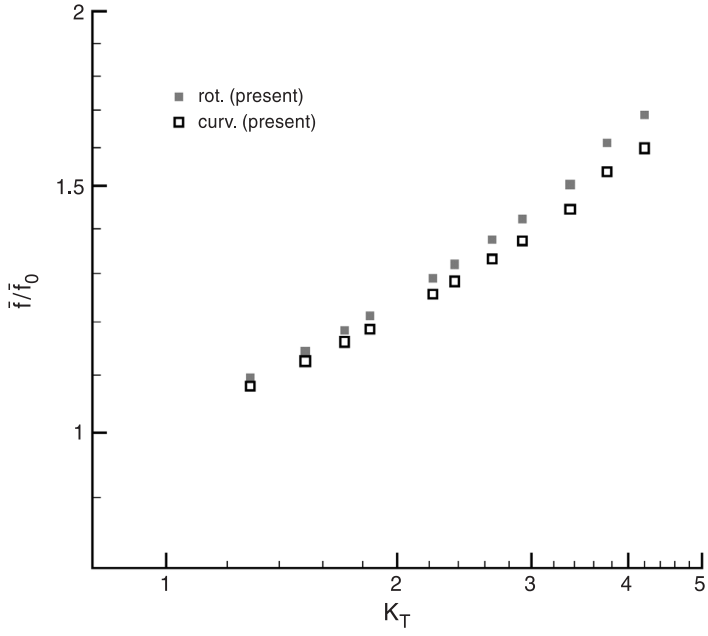

(b) Top (or bottom) side

(*Continued*)

Figure 6.
Individual sides and overall average friction factors at $Re = 20{,}000$

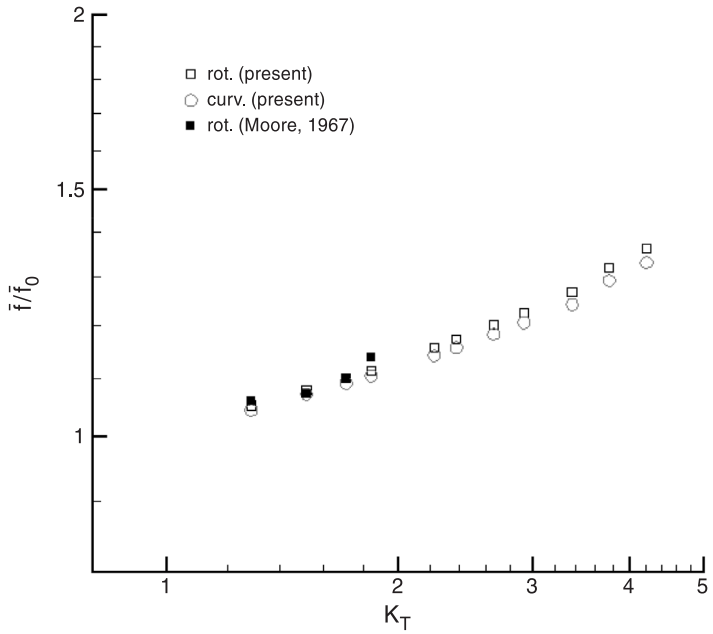

(c) Overall side

Figure 6.

with experimental data (Moore, 1967), although small discrepancies are found on the top (or bottom) side.

In order to investigate the effect of rotation or curvature on the friction factor in detail, the distribution of the local friction factor is shown in Figure 7. The magnitude of the friction factor on the top (or bottom) increases with K_{T}, while the suction side values are reduced (Figure 7(a)). This may occur because the counter-rotating eddy deflects the secondary flow toward the top (or bottom), increasing the gradients of axial velocity at the near wall. For $K_T = 3.76$, due to an additional pair of vortices induced by the flow instabilities, a sudden increase in the value of f/f_0 occurs on the pressure side, except near the symmetry line where the magnitude of f/f_0 drops considerably (Figure 7(b)).

Conclusions

Detailed numerical studies were performed using a low Reynolds number $k-\omega$ turbulence model and higher order discretization scheme in order to investigate the quantitative analogy of fully developed turbulent flow in orthogonally rotating ducts and stationary curved ducts with square cross-section. The following conclusions were made:

(1) The validity of the similarity parameters suggested by Ishigaki (1996) for circular pipe flow was confirmed for square duct flow. That is, K_{TR}

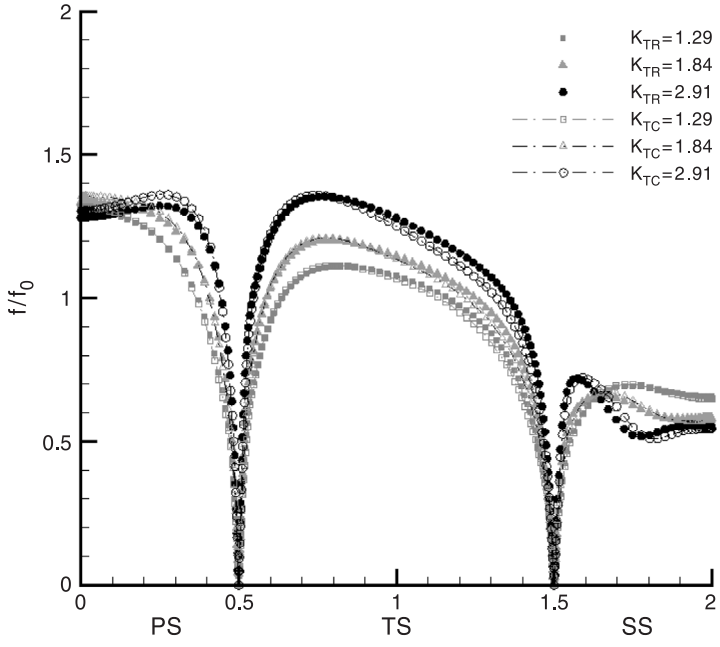

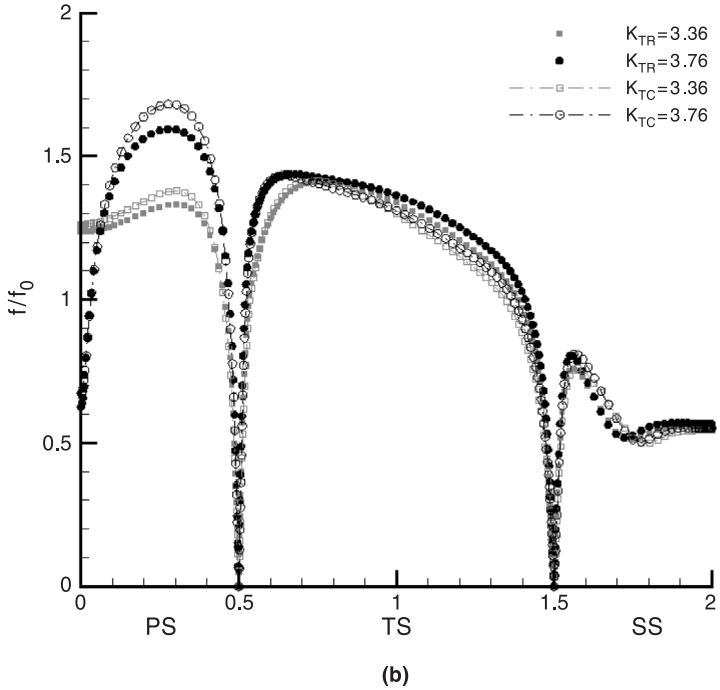

Figure 7.
Distributions of the local normalized friction factors at $Re = 20{,}000$

and Ro for the turbulent flow in orthogonally rotating ducts corresponded to K_{TC} and λ for stationary curved duct flows. Here, the hydraulic diameter, d_h, was used instead of the pipe diameter, d.

(2) For the Rossby number or curvature ratio that satisfies the "asymptotic invariance property", analogous to laminar flow, the quantitative analogy between the two flows was established clearly. Both the friction factor and the primary and secondary flow patterns were similar for a wide range of K_T.

(3) Based on this methodology, the flow characteristics in orthogonally rotating ducts can be predicted by considering the flow in stationary curved ducts, and vice versa.

The mean flow features inside rotating and curved ducts could be represented reliably using a low Reynolds number $K - \omega$ model, but more refined turbulence models (i.e. Reynolds stress model, LES) are needed to consider the non-isotropic effect of the Coriolis force and curvature on the turbulence. That investigation will be considered in a separate paper.

References

Chorin, A.J. (1968), "Numerical solution of the Navier-Stokes equations", *Math. Comp.*, 22, pp. 745-62.

Chen, H.C. and Patel, V.C. (1988), "Near-wall turbulence models for complex flows including separation", *AIAA J.*, 26, pp. 641-8.

Constantinescu, G. and Patel, V.C. (1998), "A numerical model for simulation of pump-intake flow and vortices", *J. Hydrodynamic Eng.*, 124, pp. 123-34.

Harlow, F.W. and Welch, J.E. (1965), "Numerical calculation of time-dependent viscous incompressible flow of fluids with free surface", *Phy. Fluids*, 8, pp. 2182-9.

Hill, P.G. and Moon, I.M. (1962), *Effects of Coriolis on the turbulent boundary layer in rotating fluid machines*, Report No. 69, Gas Turbine Lab., Massachusetts Institute of Technology, Cambridge, MA.

Humphrey, J.A.C., Whitelaw, J.H. and Yee, G. (1981), "Turbulent flow in a square duct with strong curvature", *J. Fluid Mech.*, 103, pp. 443-63.

Hur, N., Thangam, S. and Speziale, C.G. (1990), "Numerical study of turbulent secondary flow in curved ducts", *ASME J. Fluids Eng.*, 112, pp. 205-11.

Ishigaki, H. (1994), "Analogy between laminar flows in curved pipes and orthogonally rotating pipes", *J. Fluid Mech.*, 268, pp. 133-45.

Ishigaki, H. (1996), "Analogy between turbulent flows in curved pipes and orthogonally rotating pipes", *J. Fluid Mech.*, 307, pp. 1-10.

Ito, H. (1959), "Friction factors for turbulent flow in curved pipes", *ASME J. Basic Eng.*, 81, pp. 123-34.

Iacovides, H. and Launder, B.E. (1991), "Parametric and numerical study of fully developed flow and heat transfer in rotating rectangular ducts", *ASME J. Turbomachinery*, 113, pp. 331-8.

Ito, H. and Nanbu, K. (1971), "Flow in rotating straight pipes of circular cross section", *ASME J. Basic Eng.*, 93, pp. 383-94.

Johnston, J.P., Hallen, R.M. and Lezius, D.K. (1972), "Effects of spanwise rotation on the structure of two-dimensional fully developed turbulent channel flow", *J. Fluid Mech.*, 56, pp. 533-57.

Launder, B.E. and Spalding, D.B. (1974), "The numerical computation of turbulent flows", *Comp. Methods Applied Mech. Eng.*, 3, pp. 96-116.

Lee, G.H. and Baek, J.H. (2001), "Similarity comparison of laminar flows in an orthogonally rotating square duct and a stationary curved square duct", *Int. J. Rotating Machinery*(in press).

Lezius, D.K. and Johnston, J.P. (1976), "Roll-cell instabilities in rotating laminar and turbulent channel flows", *J. Fluid Mech.*, 77, pp. 153-75.

Lee, M.J., Oh, B.D. and Kim, Y.B. (2001), "Canonical fractional-step methods and consistent boundary conditions for the incompressible Navier-Stokes equations", *J. Comp. Phys.*, 168, pp. 73-100.

Menter, F.R. (1993), "Zonal two equation $k-\omega$ turbulence models for aerodynamic flows", AIAA-93-2906.

Moore, J. (1967), *Effects of Coriolis on turbulent flow in rotating rectangular channels*, Report No. 89, Gas Turbine Lab., Massachusetts Institute of Technology, Cambridge, MA.

Patankar, S.V., Pratap, V.S. and Spading, D.B. (1975), "Prediction of turbulent flow in curved pipes", *J. Fluid Mech.*, 67, pp. 583-95.

Rosenfeld, M., Kwak, D. and Vinokur, M. (1991), "A fractional step solution method for the unsteady incompressible Navier-Stokes /in generalized coordinate systems", *J. Comp. Phys.*, 94, pp. 102-37.

Schlichting, H. (1979), *Boundary layer theory*, 7th edition, McGraw-Hill.

Stephens, M.A. and Shih, T.I-P. (1999), "Flow and heat transfer in a smooth U-duct with and without rotation", *J. Propulsion & Power*, 15, pp. 272-9.

Song, B., Liu, G.R. and Amano, R.S. (2001), "Applications of a higher-order bounded numerical scheme to turbulent flows", *Int. J. Num. Methods Fluids*, 35, pp. 371-94.

Trefethen, L.M. (1957), *Flow in rotating radial ducts*, Report No. 55GL350-A, General Electric Company.

Taylor, A.M.K.P., Whitelaw, J.H. and Yianneskis, M. (1982), "Curved ducts with strong secondary motion: velocity measurements of developing laminar and turbulent flow", *ASME J. Fluids Eng.*, 104, pp. 350-9.

Wilcox, D.C. (1993), *Turbulence modeling for CFD*, DCW Industries.

Wilcox, D.C. (1994), "Simulation of transition with a two-eqsturbulence model", *AIAA J.*, 32, pp. 247-55.

Younis, B.A. (1993), "Prediction of turbulent flows in rotating rectangular ducts", *ASME J. Fluids Eng.*, 115, pp. 646-52.